Apoptosis (2019) 24:326–340
https://doi.org/10.1007/s10495-019-01519-x

Combination treatment of podophyllotoxin and rutin promotes mouse Lgr5^{+ve} intestinal stem cells survival against lethal radiation injury through Wnt signaling

Bhargab Kalita[1] · Rajiv Ranjan[1] · Manju Lata Gupta[1]

Published online: 6 February 2019

Abstract
It has been well established that radiation-induced gastrointestinal injury is manifested through loss of intestinal crypt stem cells and disruption of the mucosal layers, resulting in diarrhoea, weight loss, electrolyte imbalance, infection and mortality. Podophyllotoxin and rutin in combination (G-003M) has been reported to regulate endogenous cellular antioxidant defense systems and inflammatory response. However, the mechanism by which G-003M ameliorates radiation-induced intestinal stem cell (ISC) injury remains unclear. Here, we hypothesize the radioprotective potential of G-003M would amplify the intestinal crypt stem cells through upregulation of Wnt/β-catenin signaling and accelerate the reconstitution of the irradiated intestine. Our results showed significant functional and structural intestine regeneration in irradiated animals following G-003M treatment which resulted in improved animal survival. Immunohistochemical examination revealed an enhancement in Lgr5^{+ve} crypt stem cells. Increased β-catenin nuclear translocation resulted in upregulation of β-catenin target genes that supported ISC renewal and expansion in G-003M-treated mice, as compared to IR-treated mice. However, G-003M could not rescue the Wnt knockdown cohorts (XAV939 treated) which exhibited greater incidence of intestinal apoptosis, DNA damage and crypt depopulation upon radiation exposure. These findings suggest the involvement of Wnt pathway during G-003M mediated amelioration of IR-induced ISC injury. G-003M also minimised acute inflammation by restricting the infiltration of immune cells into the intestinal venules. Furthermore, G-003M treated animals showed improved anti-tumor response compared to FDA approved Amifostine. Taken together, our findings suggest that G-003M may be used as a potential countermeasure for radiation injuries as well as an adjuvant during anti-cancer therapy.

Keywords Intestine · Ionising radiation · Stem cells · Podophyllotoxin · Rutin · Radiation protection

Introduction

Rapidly renewed tissues such as gastro-intestinal (GI) tract and haematopoietic system are the most sensitive organs in the human body to radiation induced apoptosis. Gastrointestinal injury is the primary limiting factor in pelvic and abdominal radiotherapy, but no effective treatment is available currently. Ionising radiation usually strikes the intestinal crypts where stem cells are positioned in their functional state. These adult stem cells are primarily responsible for tissue regeneration and homeostasis following lethal radiation damage. Previous genetic studies in mice evidently demonstrated that intestinal stem cells (ISCs) are represented by Lgr5 [1], CD133/Prominin 1 [2], and Bmi-1 [3] expressing cells at the crypt base. The putative multipotent, ISC is located at the crypt base, either at fourth or fifth cell position from the base [4] or as crypt base columnar cells [5]. Following radiation exposure, crypt base cells undergo cell cycle arrest or rapid apoptosis. The degree of intestinal damage and cell loss is proportional to the radiation dose [6]. Following radiation injury, the crypt becomes "non-viable" and dies out within 48 h. However, one or more surviving ISC can rapidly proliferate to regenerate the crypt within 72–96 h. Therefore, repopulation of clonogenic proliferating crypt cells by ISCs play a determining role in deciding the fate of a damaged crypt after injury. Thus, GI protection is a significant support for medical management not only

✉ Manju Lata Gupta
manjugupta@inmas.drdo.in

[1] Division of Radioprotective Drug Development and Research, Institute of Nuclear Medicine and Allied Sciences, Brig. S. K. Majumdar Marg, Timarpur, Delhi 110054, India

in case of radiotherapy but also during accidental radiation exposures [7].

The Wnt/β-catenin signaling pathway plays a pivotal role in regulating the proliferation and differentiation of the clonogenic stem cells progenitors during the crypt–villus renewal and maturation process [8]. Hence, agents that upregulates the β-catenin/T cell factor (TCF) signal transduction pathway might help in early recovery from radiation injury through increased stem cell proliferation that give rise to more rapidly dividing transit cells/colony forming cells [9, 10].

Numerous therapeutic strategies have been examined to alleviate radiation induced intestinal damage. However, majority of them were unsuitable for human use [11] due to their toxic behaviour. Low molecular weight compounds such as vitamin E and its derivatives (Tocopherol mono glucoside) [12], ascorbic acid, polyphenols, glutathione etc. were also found to have good radioprotective ability which has been due to their anti-oxidant property. Out of thousands agents explored, synthetic thiol Amifostine (Ethyol) is the only compound which is permitted by US FDA for specific use as adjuvant in radiotherapy [13]. However, its high toxicity, unfavourable routes of administration, and narrow protection time window has significantly diminished its effectiveness in clinical applications [14, 15].

Exploring natural resources for countering the deleterious effects of radiation has become one of the most promising themes primarily due to its potent anti-oxidant and anti-inflammatory properties [16, 17]. The whole extract and semi purified fractions derived from *Podophyllum hexandrum* were found to confer significant survival benefits to lethally irradiated rodent models [18, 19]. After observing radio protective potential in various solvent extracts, we isolated active molecules from *Podophyllum hexandrum* rhizomes and chemically characterized them [20]. On performing their bioactive characteristics against radiation we observed that a combination of two isolated active principles (podophyllotoxin and rutin) could effectively modulate radiation induced inflammation, oxidative stress and apoptosis in mice intestine [21]. Radiation injury caused to mice lungs [22] and hematopoeitic systems [23] were also minimized. However, the mechanism of G-003M mediated ISC renewal and reconstitution of progenitor's lineages during radiation injury remained elusive.

Hence, the present study was designed to assess the constructive role of G-003M during intestinal tissue reconstitution and its functionality following radiation injury. The focus of the study is to understand the mechanism of G-003M mediated ISC renewal and expansion after radiation injury. The study includes G-003M mediated modulation in Lgr5 responsive ISCs localization and its differentiation through β-catenin transactivation of various Wnt target genes. Abrogation of Wnt/β-catenin pathway by small molecule inhibitor XAV939 was envisaged to confirm the role of Wnt during G-003M mediated intestinal protection. Further, the regulation of inflammatory entities like ICAM-1 and VCAM-1 and its role in recruitment of immune cells (Gr-1, CD-3 and CD-19) into the intestinal venules were also explored. Caspase-3 activity and cell death was also evaluated. Additionally, comparative potential of G-003M versus Amifostine in cancer radiotherapy for differential protection in tumor bearing mice model was also envisaged. Based on the above findings, we ascertain that G-003M is protective against radiation induced intestinal injury and found that Wnt signaling is the key pathway involved in intestinal recovery from radiation injury.

Results

G-003M blocked the infiltration of Gr-1$^+$, CD3$^+$ and CD19$^+$ immune cells through modulation of ICAM-1 and VCAM-1 expression

Radiation induced inflammatory response is mainly initiated by the infiltration of immune cells into the intestinal endothelium. Persistence of these immune cells ultimately leads to chronic inflammation in the gut. Immuno-fluorescence studies (Fig. 1a–d) revealed significant increase in infiltration of Gr-1$^+$ (> 20-fold, $p < 0.001$), CD-3$^+$ (> twofold, $p < 0.001$) and CD-19$^+$ (> 2.5-fold, $p < 0.001$) expressing inflammatory immune cells into the small intestinal venules at day 1 post 9 Gy TBI compared to the untreated group. However, G-003M administration restricted the recruitment of these inflammatory responsive cells Gr-1$^+$ (> twofold, $p < 0.001$), CD-3$^+$(> 1.5-fold, $p < 0.001$) and CD-19$^+$ (> 1.5-fold, $p < 0.001$) into the intestinal sites as compared to the IR-treated group. Importantly, the effect of G-003M + Bay 11-7082 + IR combinatorial treatment was analogous to the G-003M + IR cohorts and led to further suppression of immune cells infiltration Gr-1$^+$ (> 3.5-fold, $p < 0.001$), CD-3$^+$ (> twofold, $p < 0.001$) and CD-19$^+$ (> twofold, $p < 0.001$) into the intestinal endothelium as compared to the irradiated group (Fig. 1a–d).

Since adhesion molecules are well reported to participate in mediating the pathogenesis of inflammatory cell directed tissue injury, we examined the expression of ICAM-1 and VCAM-1 in mice jejunum of different treatment groups post-irradiation. Following day 1 of 9 Gy TBI, a significant induction (> 2.5-fold, $p < 0.001$) of ICAM-1 expression was evident in the irradiated mice intestine compared to the untreated group (Fig. 1e, f). Whereas, a marginal increase in VCAM-1 expression was observed at day 1 post-TBI (Fig. 1e, g). G-003M treatment not only down regulated ICAM-1 expression by (> 1.5-fold, $p < 0.001$) but could also restore the baseline levels of VCAM-1 at day 1 as

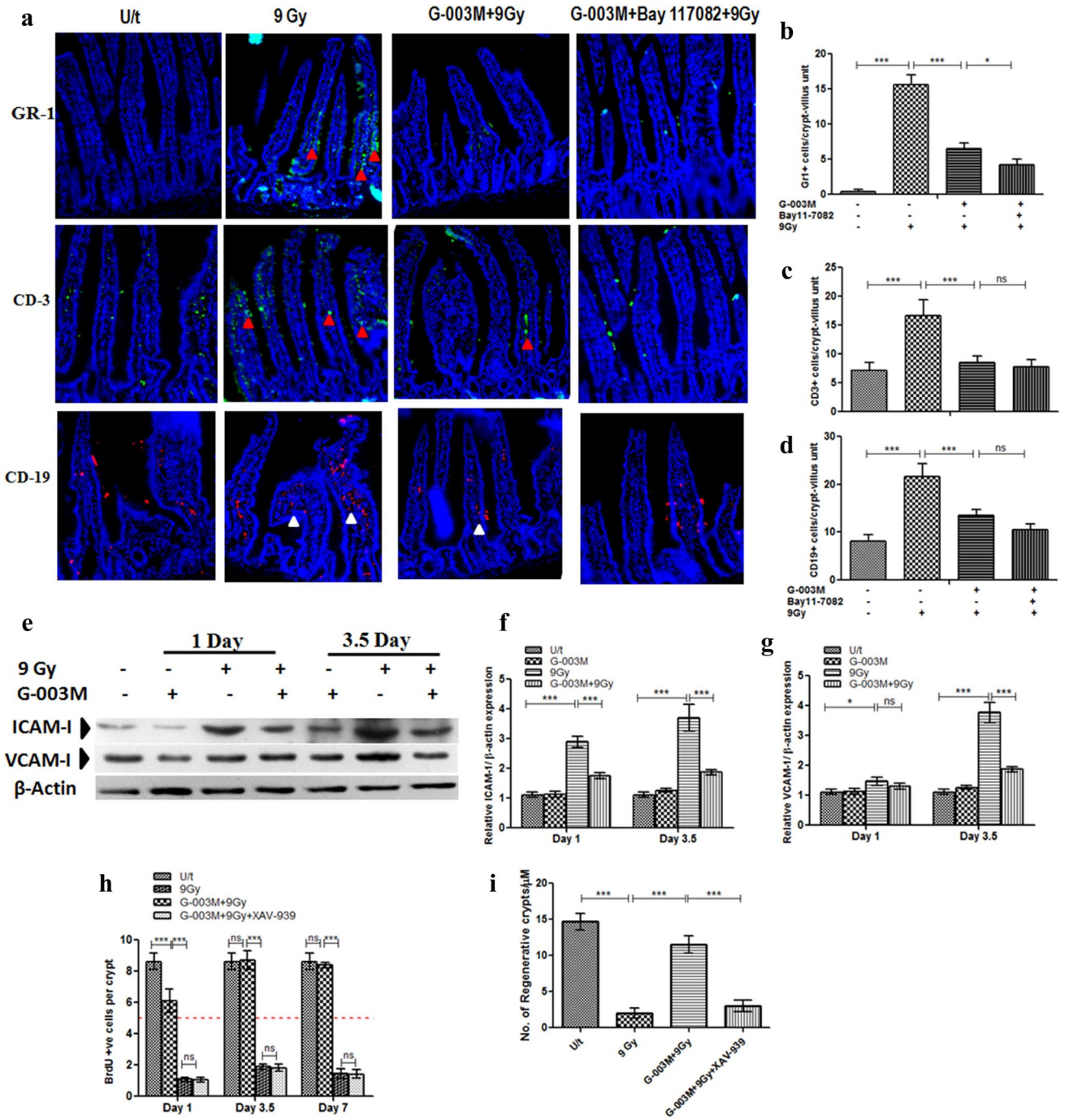

Fig. 1 G-003M reduces radiation induced inflammation and augments crypt proliferation in the mice intestine. **a** Immunofloures-cence (IF) staining was performed in C57BL/6 mice jejunum using Gr-1$^+$ (FITC) (red arrow heads), CD3$^+$ (FITC) (red arrow heads) and CD19$^+$ (PE) (white arrow heads) at 24 h post-irradiation. Proximal jejunum was taken from mice (n = 3/group) that were left untreated (U/t), or exposed to 9 Gy TBI, or given G-003M prior to 9 Gy TBI 60 min or G-003M + Bay117082(G-003M + Bay117082 + 9Gy) for IF staining. Green fluorescence indicates Gr-1$^+$ and CD3$^+$ cells. Red fluorescence indicates CD19$^+$ cells. Nuclei of cells were stained with 4′,6′-diamidino-2-phenylindole (DAPI, blue). Quantification of staining of **b** Myeloid lineage Ly-6G (Gr-1), **c** Cd3e (T-cell), **d** Cd19 (B cell), **e** After Day 1 and Day 3.5, mice were sacrificed and intestinal protein extracts were prepared and assayed by immunoblotting for ICAM-1 and VCAM-1 expression. Quantification of the expression of **f** ICAM-1, **g** VCAM-1 normalised to β-actin. **h** BrdU-positive cells were scored in ten complete, well-oriented cross sections for each animal. Dashed red line: number of BrdU-positive cells considered critical for crypt survival, **i** Quantification of regenerative crypts in mice (n = 3) of different treatment groups. Representative micrographs were taken at ×20 magnification. A value of $p < 0.05$ is considered statistically significant. ns = nonsignificant, *$p < 0.05$, **$p < 0.01$, ***$p < 0.001$. (Color figure online)

compared to IR-treated group (Fig. 1e–g). By 3.5 days post 9 Gy TBI, expression of both ICAM-1 and VCAM-1 was found enhanced by (> 3.5-fold, $p < 0.001$) and (> 3.5-fold, $p < 0.001$) respectively compared to the untreated animals. Interestingly, G-003M treatment resulted in further down-regulation of ICAM-1 and VCAM-1 expression in the mice intestine by > twofold ($p < 0.001$) and > twofold ($p < 0.001$) respectively compared to the irradiated group of animals (Fig. 1e–g). G-003M (alone) did not induce any significant changes in the expression of ICAM-1 and VCAM-1 and was comparable to the untreated groups at all the time-points of study.

G-003M augmented intestinal crypt proliferation after TBI

It is well reported that exposure to radiation doses of > 8 Gy induces cell cycle arrest and apoptosis of the crypt epithelial cells within 24 h. This leads to depletion of regenerative crypts by 3.5 days and eventually villi denudation by 7 days post-irradiation in mice [24]. Henceforth, we evaluated the histological alterations of radiation-induced GI injury and the countering effect of G-003M at 1, 3.5 and 7 days, post 9 Gy exposure. Firstly, we examined whether G-003M induces crypt stem cells proliferation in mice receiving 9 Gy TBI. Following 9 Gy TBI, the number of $BrdU^{+ve}$ cells per crypt decreased by > sixfold ($p < 0.001$) at day 1, > 3.5-fold ($p < 0.001$) at 3.5 days and > fourfold ($p < 0.001$) by 7 days as compared to untreated mice (Fig. 1h). Consequently this led to significant depletion of regenerative crypts at 3.5 day by > 5.5-fold ($p < 0.001$) compared to untreated control (Fig. 1i). In contrast, G-003M treatment resulted in amplification of $BrdU^{+ve}$ cells per crypt at 1 day (> 60%, $p < 0.001$), 3.5 days (> 75%, $p < 0.001$) and 7 days (> 70%, $p < 0.001$) compared to 9 Gy treated groups post-TBI (Fig. 1h). The percentage of regenerative and viable crypts were found significantly enhanced after G-003M treatment compared with irradiated group (G-003M + 9Gy, 75 ± 2.27 vs. 9 Gy 20 ± 2.04; $p < 0.001$) at 3.5 days following 9 Gy exposure (Fig. 1i). However, the combinatorial treatment (G-003M + XAV-939 + 9Gy) led to significant ($p < 0.001$) depletion of $BrdU^{+ve}$ cells per crypt resulting in diminished regenerative potential at all the time-points of study as compared to (G-003M + 9Gy) treated group (Fig. 1h, i) .

The irradiated jejunum of C57BL/6 mice demonstrated pathological features of severe radiation damage after day 3.5 and day 7 of lethal radiation exposure (9 Gy). Disruption of mucosal barrier, denuded villi, non-viable crypts, decrease in mean crypt–villus height was observed in the irradiated group. These histological alterations were minimised by G-003M treatment. By day 7, significant presence of viable crypts, intact villi and mucosal layers was evident in the G-003M treated group. However, G-003M could not retain its radioprotective potential in the XAV939 treated cohorts at both 3.5 and 7 days (data not shown). The regenerative potential of the crypts treated with (G-003M + XAV939 + IR) was found severely compromised compared to the G-003M + IR treatment at all the time-points of study (Fig. 1h, i).

G-003M upregulates Wnt signaling in lethally irradiated mice intestine

To understand the possible mechanism by which G-003M enhances crypt regeneration following 9 Gy irradiation, we examined the expression of Wnt signals in the mice intestine. At 3.5 days, immunoblot analysis indicated reduction of Wnt expression by > 2.5-fold ($p < 0.001$) in mice exposed to 9 Gy γ-irradiation, when compared to untreated group. This reduction of Wnt expression in the gut epithelium was countered by > eightfold ($p < 0.001$) upon G-003M administration at 3.5 days. By 7 days of 9 Gy exposure, expression of Wnt decreased by > 1.5-fold in comparison to the untreated mice. G-003M treatment resulted in further upregulation of Wnt signals by > sixfold ($p < 0.001$) at 7 days compared to the irradiated group (Fig. 2a, b). In contrast, G-003M administration could not restore Wnt levels in (G-003M + XAV-939 + 9Gy) group at 3.5 Days thereby leading to lesser crypt regeneration. No significant variation in the expression pattern of Wnt was found in the G-003M (alone) group at all the time-points of study (Fig. 2a, b). Thus, our findings strongly suggest that G-003M enhances crypt regeneration by upregulating Wnt signals in the mice intestine.

G-003M amplified the $Lgr5^{+ve}$ expressing ISCs population in mice crypts

Western blot analysis revealed reduction of Lgr5 expression in mice jejunum at day 1 (> 10-fold, $p < 0.001$), 2 days (> 10-fold, $p < 0.001$), 3.5 days (> 2.5-fold, $p < 0.001$) and 7 days (> 3.5-fold, $p < 0.001$) following 9 Gy exposure as compared to untreated group (data not shown). G-003M pre-treatment significantly maintained Lgr5 expression in the lethally irradiated mice crypts at day 1 (> 3.5-fold, $p < 0.001$), day 2 (> fivefold, $p < 0.001$) and by 3.5 days (> 2.5-fold, $p < 0.001$), 7 days (> threefold, $p < 0.001$) as compared to corresponding IR-treated (alone) group (Fig. 2c, d). In agreement with this observation, immunoflourescence staining of jejunum crypts revealed a significant ($p < 0.001$) enhancement in the number of Lgr5-expressing ISCs in the G-003M treated mice. Though at 3.5 days following 9 Gy TBI, the $Lgr5^{+ve}$ crypt stem cells were found reduced in the irradiated mice, yet these cells remain amplified in G-003M-treated mice. These observations signify protection from radiation injury via expansion of the crypt

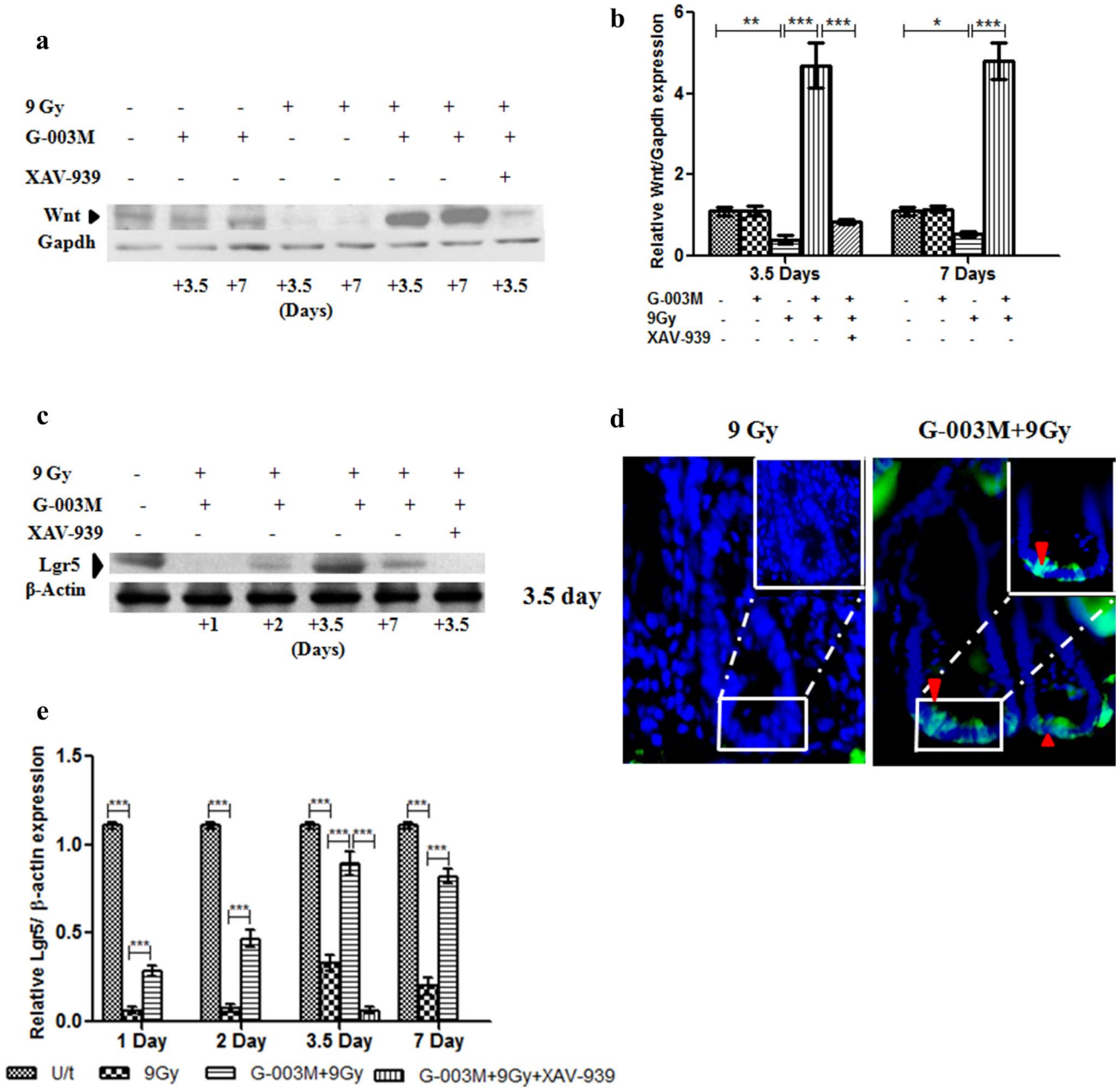

Fig. 2 G-003M upregulates Wnt contributing to amplification of Lgr5$^+$ ISCs in mice intestine **a** After 3.5 and 7 Days, mice were sacrificed and intestinal protein extracts were prepared and assayed by immunoblotting for Wnt expression. **b** Quantification of Wnt expression was normalised to Gapdh expression, using IMAGE lab software for densitometry. **c** Day 1, 2, 3.5 and 7 following differential treatments, mice were sacrificed and intestinal protein extracts were prepared and assayed by immunoblotting for Lgr5 expression **d** Immunoflourescence (IF) staining was performed in C57BL/6 mice jejunum using Lgr5 (FITC) (red arrow heads) at 3.5 days post-irradiation. Proximal jejunum was taken for IF staining. Green flourescence indicates Lgr5$^+$ ISCs. Nuclei of cells were stained with 4′, 6′-diamidino-2-phenylindole (DAPI, blue) **e** Quantification of Lgr5 expression was normalised to β-actin expression, using IMAGE lab software for densitometry. A value of $p<0.05$ is considered statistically significant. ns = nonsignificant, *$p<0.05$, **$p<0.01$, ***$p<0.001$. (Color figure online)

stem cell compartment (Fig. 2e). By 7 days, the number of Lgr5$^{+\,ve}$ ISCs was restored to baseline levels in the G-003M pre-treated mice (Fig. 2c). In contrast, the combined treatment (G-003M + XAV939 + 9Gy) resulted in significant ($p<0.001$) decline of Lgr5 expression leading to diminished crypt stem cell expansion compared to (G-003M + 9Gy) treatment groups at 3.5 days post TBI (Fig. 2c–e).

G-003M stimulated the nuclear translocation of β-catenin in mice jejunum crypts

Previous reports have indicated the critical role played by β-catenin signaling in maintaining intestinal homeostasis [8]. Under resting state, β-catenin is localized to the cytoplasm. While Wnt activation results in its translocation from the cytoplasm to the nucleus. Inside the nucleus, β-catenin binds to the TCF/LEF transcription factor complex and transactivates the expression of Wnt-target genes. Henceforth, we examined the relative quantities of β-catenin in the cytoplasm and nucleus of intestinal crypts from different TBI irradiated groups with or without G-003M treatment. Western blot analysis did not demonstrate any increase in nuclear β-catenin levels at 1 day, 2 days, 3.5 Days and 7 Days of the lethally (9 Gy) irradiated mice compared to untreated control groups (data not shown). In contrast, the nuclear/cytosolic expression ratio of β-catenin started to rise in G-003M treated mice at day 1 (> twofold, $p < 0.001$), which further increased by > 3.5-fold at day 2 compared to IR-treated animals. The expression ratio peaked around 3.5 days (> sixfold, $p < 0.001$) after which a marginal fall was noticed at day 7 (> fourfold, $p < 0.001$) (Fig. 3a, c). Immunofloures-cence microscopy also confirmed a significant ($p < 0.001$) increase in nuclear β-catenin staining in the crypt progenitor cells in G-003M-treated animals at 3.5 days (Fig. 3b). Our results suggest that G-003M enhanced the stabilization and nuclear translocation of β-catenin in the intestinal crypt cells. However, G-003M could not induce nuclear β-catenin levels in the (G-003M + XAV-939 + 9Gy) combined treated group of animals as compared to (G-003M + 9Gy) group (Fig. 3a–c).

To explore the possibility whether the unrestrictive effect of G-003M on β-catenin was due to its suppression of DKK1, the level of DKK1 was determined by western blot analysis. Exposure to 9 Gy led to induction (> 2.5-fold, $p < 0.001$) of DKK1 in mice intestine compared to the untreated control group (Fig. 3d, e). Importantly, we observed that G-003M pre-treatment inhibited the DKK1 expression (~ twofold, $p < 0.001$) at 3.5 days in mice gut epithelium, following lethal dose (9 Gy) of γ-irradiation. Surprisingly, G-003M + XAV939 + 9Gy treatment significantly induced the expression of DKK1 by > 1.5-fold ($p < 0.001$) compared to G-003M + 9Gy thereby leading to restricted β-catenin translocation in mice intestinal crypt (Fig. 3d, e).

G-003M upregulates the expression of β-catenin target effectors in lethally exposed mice intestine

Since β-catenin regulates an array of genes involved in crypt survival during radiation exposure, we examined the expression of c-Myc, Survivin and Nanog in mice jejunum of different treatment groups. Exposure to 9 Gy radiation led to suppression of c-Myc (> twofold, $p < 0.001$), Survivin (> 3.5-fold, $p < 0.001$) and Nanog (> 2.5-fold, $p < 0.001$) expression at 3.5 days in the mice gut compared to untreated groups (Fig. 3d, e).

Importantly, G-003M counteracted the effects of radiation by upregulating the expressions of c-Myc (> 2.0-fold, $p < 0.001$), Survivin (> 2.5-fold, $p < 0.001$) and Nanog (> 2.5-fold, $p < 0.001$) essential for crypt stem cell survival and expansion (Fig. 3d, e). However, the expression of c-Myc, Survivin and Nanog were found significantly ($p < 0.001$) reduced in the (G-003M + XAV-939 + 9Gy) treated animals as compared to (G-003M + 9Gy) treated group. The levels of c-Myc, Survivin and Nanog remained unchanged in the G-003M (alone) treatment group and was comparable to the untreated animals (Fig. 3d, e).

G-003M minimises IR induced apoptosis in mice intestine

To evaluate crypt apoptosis, in situ TUNEL staining was performed. The irradiated mice showed a > sixfold ($p < 0.001$) increase in TUNEL-positive cells (TPC) per crypt region as compared to untreated animals (Fig. 4a, b). However, G-003M administration resulted in reduction (> 2.0-fold, $p < 0.001$) of TUNEL-positive cells when compared to the lethally irradiated group (Fig. 4a, b). Interestingly, G-003M could not rescue the intestinal crypts of (G-003M + XAV-939 + 9Gy) group from radiation induced apoptosis. Marked increase of TUNEL-positive cells by > twofold ($p < 0.001$) was evident in the (G-003M + XAV-939 + 9Gy) group compared to (G-003M + 9Gy) group (Fig. 4a, b).

To understand the possible mechanism by which G-003M inhibits apoptosis following 9 Gy irradiation, we evaluated the expression of active Caspase-3 in the mice intestine. Exposure to 9 Gy radiation led to induction (> 2.5-fold, $p < 0.001$) of active Caspase-3 expression in mice jejunum when compared to untreated group of animals (Fig. 3d, e). This radiation induced escalation of active Caspase-3 levels were countered by G-003M treatment by > 2.5-fold ($p < 0.001$) (Fig. 3d, e). However, G-003M could not restore the active Caspase-3 levels of (G-003M + XAV939 + 9Gy) group to normal baseline expression. Caspase-3 activity was found enhanced by > 2.5-fold ($p < 0.001$) in the (G-003M + XAV-939 + 9Gy) group compared to (G-003M + 9Gy) treated group. G-003M (alone) treatment did not induce any change in normal baseline levels of Caspase-3 in the mice jejunum (Fig. 3d, e).

G-003M inhibits radiation induced DNA damage in intestinal crypts

Radiation induced DNA damage mainly initiates through phosphorylation of γ-H2AX, which occurs rapidly after

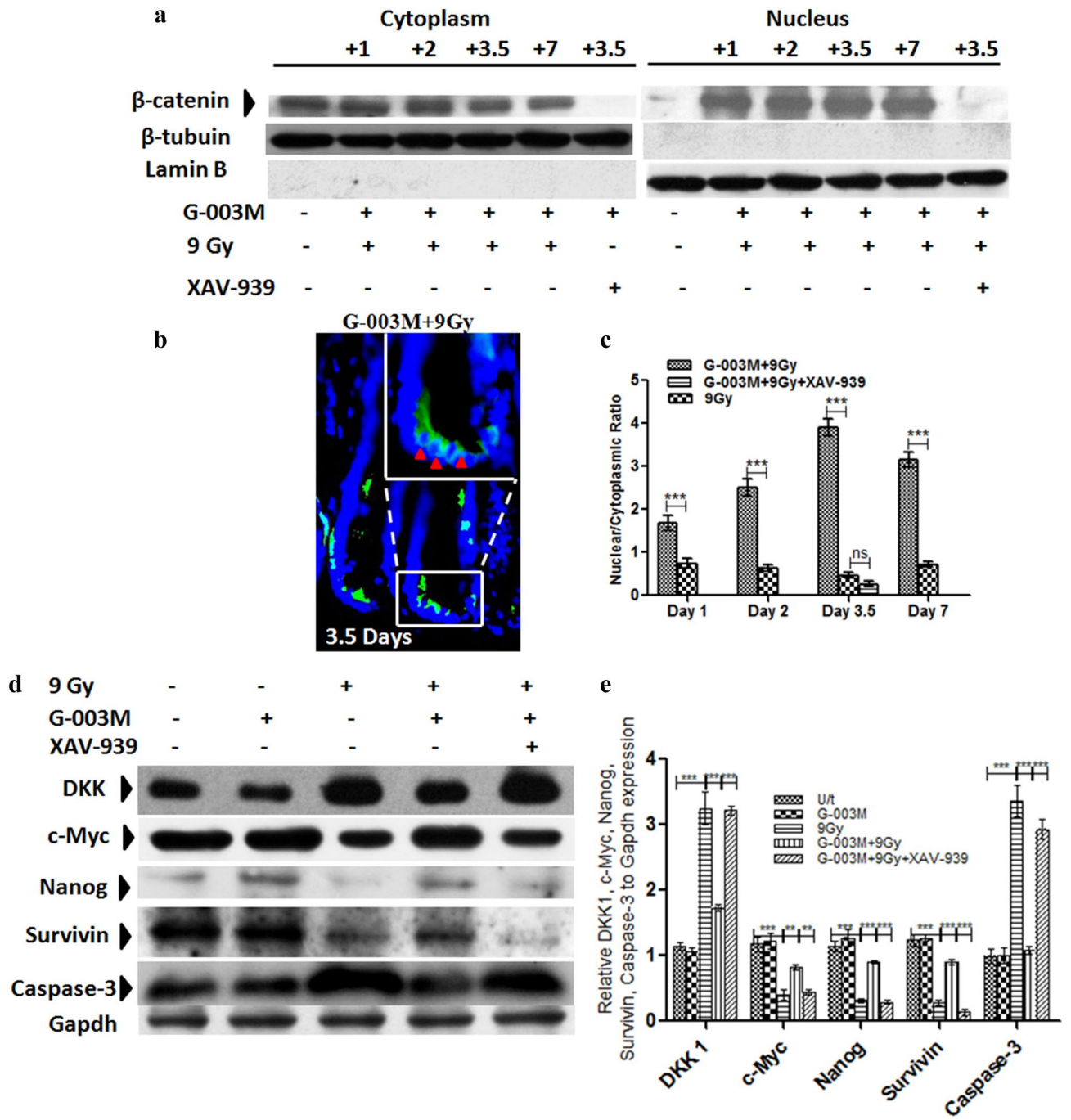

Fig. 3 G-003M mobilized β-catenin nuclear translocation upregulating Wnt target effectors in mice intestinal crypts. **a** After day 1, 2, 3.5 and 7, mice were sacrificed and intestinal nuclear and cytoplasmic protein extracts were prepared and assayed by immunoblotting for β-catenin expression. **b** Immunoflourescence staining was performed in C57BL/6 mice jejunum using β-catenin (FITC) (red arrow heads) at 3.5 days post-irradiation in (G-003M + 9Gy) treated group. Proximal jejunum was taken for IF staining. Green flourescence indicates β-catenin expression. Nuclei of cells were stained with 4′,6′-diamidino-2-phenylindole (DAPI, blue). **c** Corresponding nuclear:cytoplasmic ratios of β-catenin localisation at days (1, 2, 3.5 and 7) in differentially treated C57BL/6 mice was quantified by IMAGE J software and expressed as mean ± SD. Quantification of β-catenin expression was normalised to β-tubulin expression in the cytoplasmic and Lamin B expression in the nuclear extracts, using IMAGE lab software for densitometry. **d** Following differential treatments at day 3.5, mice were sacrificed and intestinal protein extracts were prepared and assayed by immunoblotting for Dkk1, c-Myc, Nanog, Survivin and Caspase-3 expression. **e** Quantification of Dkk1, c-Myc, Nanog, Survivin and Caspase-3 expression expression was normalised to Gapdh expression, using IMAGE lab software for densitometry. A value of $p < 0.05$ is considered statistically significant. ns = nonsignificant, *$p < 0.05$, **$p < 0.01$, ***$p < 0.001$. (Color figure online)

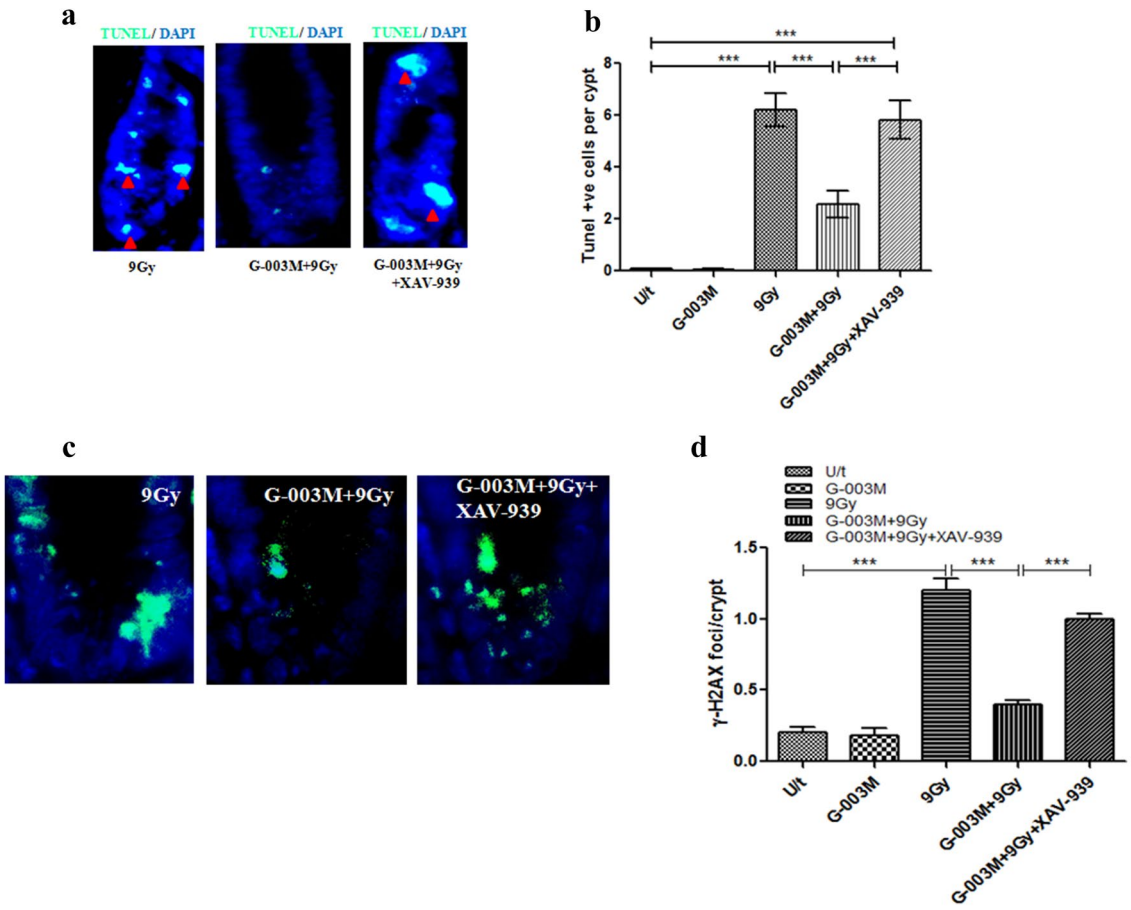

Fig. 4 G-003M minimises IR induced apoptosis and DNA damage in mice intestine. **a** Terminal deoxynucleotidyl transferase–mediated deoxyuridine triphosphate nick end labeling (TUNEL) staining was performed in 6–8 weeks old C57BL/6 mice jejunum using TUNEL Apoptosis detection kit at 3.5 days post-irradiation. Proximal jejunum was taken from mice (n = 3 group) that were differentially treated for TUNEL staining. Green flourescence indicates apoptotic cells (red arrowheads). Nuclei of cells were stained with 4′, 6′-diamidino-2-phenylindole (DAPI, blue). Representative micrographs were taken at ×40 magnification. **b** Quantification of TUNEL-positive cells (red arrowheads) per crypt of mice exposed to different treatments. **c** Immunoflourescence staining was performed in C57BL/6 mice jejunum using γ-H2AX (FITC) (red arrow heads) at 4 h post-irradiation. Proximal jejunum was taken for IF staining. Green flourescence indicates γ-H2AX foci. Representative micrographs were taken at ×40 magnification. **d** Quantification of γ-H2AX foci per crypt of mice exposed to different treatments. A value of $p < 0.05$ is considered statistically significant. ns = nonsignificant, *$p < 0.05$, **$p < 0.01$, ***$p < 0.001$. (Color figure online)

radiation exposure. The degree of DNA damage depends on the radiation dose. We found that exposure to 9 Gy resulted in significant ($p < 0.001$) increase in number of γ-H2AX foci in the intestinal crypts when compared to sham-irradiated controls at 4 h time-point post-TBI. The generation of γ-H2AX foci was significantly ($p < 0.001$) neutralized upon G-003M treatment as compared to irradiated group (Fig. 4c, d). However, G-003M could not restrict the γ-H2AX foci formation in the (G-003M + XAV-939 + 9Gy) group as compared to (G-003M + 9Gy) treated group.

G-003M is marginally more effective than amifostine in arresting tumor growth

Our previous studies have shown that G-003M did not reduce the radiosensitivity of tumor tissues [21]. Here, on a similar line, we evaluated the effectiveness of G-003M versus Amifostine in arresting tumor growth in focally irradiated tumor bearing mice. Groups of the mice were injected with G-003M (− 1 h) or Amifostine (− 30 min) before each radiation treatment. The model used was

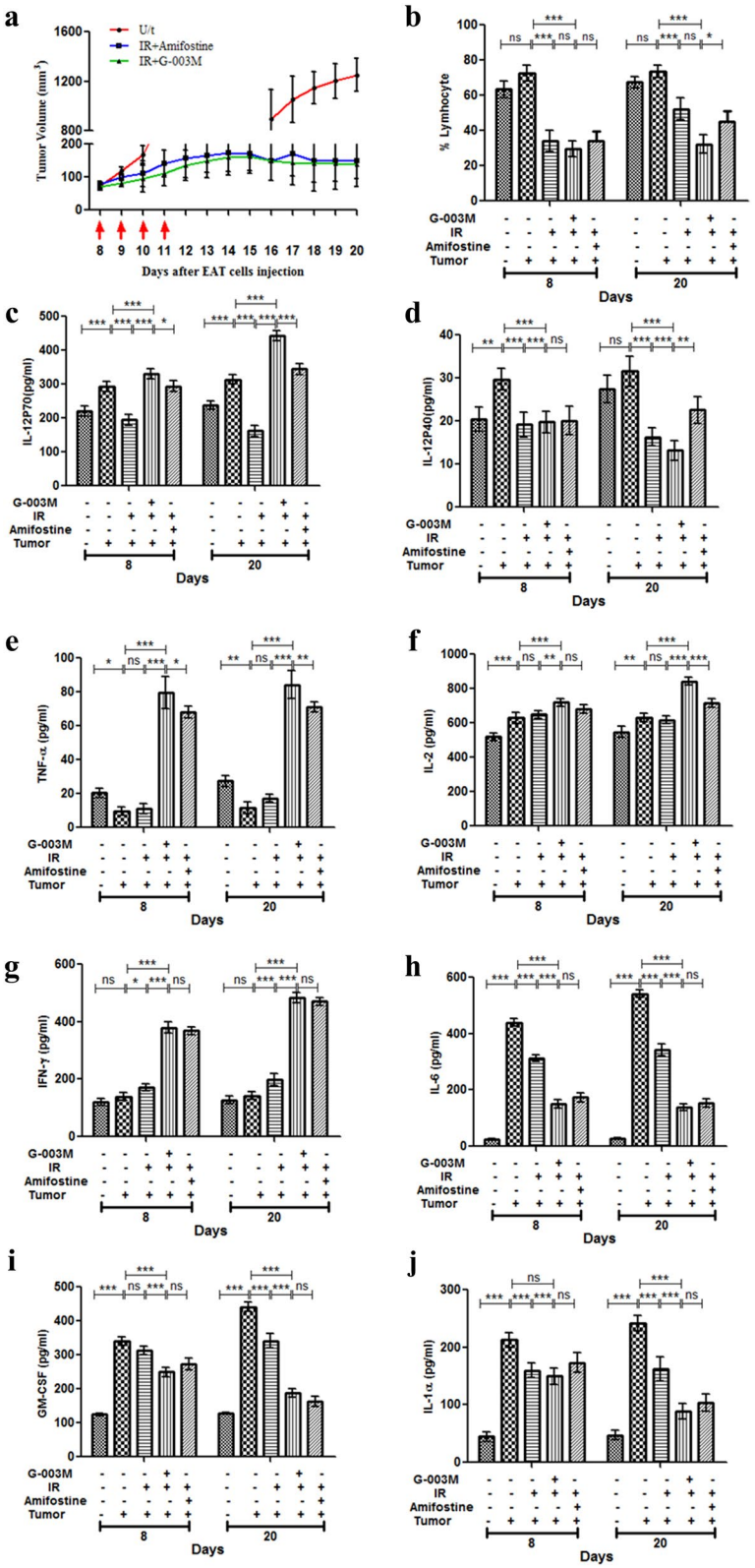

Fig. 5 G-003M is more effective than Amifostine in arresting tumor growth **a** Swiss albino 'Strain A' mice carrying EAT tumors (six mice/group) were treated with DMSO alone (U/t, untreated control) in red, G-003M (6.5 mg/kg i.m. per injection) with 10 Gy radiation (IR + G-003M) depicted in green, Amifostine (150 mg/kg i.p. per injection) with 10 Gy radiation (IR + Amifostine) depicted in blue. All treatments were applied on days 8, 9, 10 and 11 after EAT cell injection (red arrows). Tumor volume was measured every consecutive day. Values are medians of tumor volumes with error bars indicating S.D. Variation in tumor growth rate among groups were analyzed by two-way repeated measures ANOVA and by Student's t test (two-tailed, unequal variances). Estimation of **b** % Lymphocytes in peripheral blood of different treatment groups. After isolation of blood serum at different time points (8 days, 20 days) following 10 Gy γ-irradiation, serum levels of **c** IL-12P70 and **d** IL-12P40, **e** TNF-α, **f** IL-2 and **g** IFN-γ, **h** IL-6, **i** GM-CSF and **j** IL-1α cytokines (pg/ml) in different treatment groups was determined by flow cytometry using respective BD™ Cytometric Bead Array (CBA) Flex Set. A value of $p < 0.05$ is considered statistically significant. ns = nonsignificant, *$p < 0.05$, **$p < 0.01$, ***$p < 0.001$. (Color figure online)

Ehrlich ascites tumor (EAT) cells implanted in Swiss Albino 'Strain A' mice and grown subcutaneously. The antitumor effect of focal radiation was measured in the form of significant ($p < 0.001$) delay in tumor growth in both the treated groups (Fig. 5a). Interestingly, we observed that the combination treatment (G-003M + 10Gy) was marginally more effective than (Amifostine + 10Gy) in arresting tumor growth.

G-003M induces lympho-depletion essential for cancer cure

Numerous reports have asserted that during the process of cancer progression, inflammation is caused due to recruitment of different subclasses of lymphocytes at the tumor site as well as in the peripheral bloodstream [25]. This lymphodepletion phenomenon assists in generating a antitumor immune response and supports reduction in inflammation. On a similar line, we found reduction in percent lymphocytes following the treatments at 8 days, with the highest ($p < 0.001$) depletion recorded in the G-003M + 10Gy combination group compared to tumor alone group (Fig. 5b). Amifostine treatment also exhibited a similar pattern of lymphocyte depletion after 8 days (Fig. 5b). However, 20 days after the treatment mice with G-003M administration showed a significantly ($p < 0.05$) higher level of lymphocyte depletion as compared to Amifostine group (Fig. 5b). These results suggest that G-003M induces a greater extent of lympho-depletion than Amifostine which might possibly help in reducing inflammation and generating anti-tumor response necessary for cancer cure.

G-003M induces Th1 immunity essential for anti-tumor response

Several immune responsive cells like neutrophils and macrophages are responsible for the secretion of the pleiotropic cytokine IL-12 that assists in the differentiation of Th0 cells to Th1 cells [26–28]. Likewise, at 8 days a significant ($p < 0.05$) increase in IL-12 P70 levels was observed in the combined treatment (G-003M + 10Gy) as compared to (Amifostine + 10Gy) group (Fig. 5c), and the levels were found differentially ($p < 0.001$) expressed in (G-003M + 10Gy) and (Amifostine + 10Gy) at 20 days after the treatment (Fig. 5c). Furthermore, the levels of IL-12P40 were observed to be inversely linked with the levels of IL-12 P70 in both the combined treatment groups. At day 8, IL-12P40 levels were marginally down regulated in both the combination treatment groups, but by 20 days significant ($p < 0.01$) differential levels of IL-12P40 was noted in the G-003M + 10Gy versus Amifostine + 10Gy groups, opposite to IL-12 P70 levels (Fig. 5d).

At day 8 and 20, the Th1 cytokine profile analysis showed a significant up-regulation of TNF-α ($p < 0.001$), IL-2 ($p < 0.05$) and IFN-γ ($p < 0.001$) (Fig. 5e–g) in the G-003M + IR treatment as compared to IR treated tumor bearing mice. Amifostine + IR also upregulated a similar extent of Th1 cytokine levels compared to the IR treated group. However, the combined treatment of G-003M + IR induced a higher level of TNF-α ($p < 0.01$) and IL-2 ($p < 0.001$) compared to Amifostine treated cohorts at day 20. The IFN-γ level remained unchanged in both the combined treatment groups (Fig. 5e–g). These findings suggested the role of IL-12 for inducing a Th1 biased immunity.

G-003M reduces inflammatory response in tumor bearing mice

Pathogenesis of tumor induced inflammation is potentiated by several cytokines. Under chronic condition, tumor induced inflammation leads to carcinogenesis [29]. At 8 days, we observed a significant ($p < 0.001$) down regulation of pro-inflammatory cytokines (IL-6) with 10 Gy alone and both the combined treatment groups as compared to the untreated tumor bearing mice. By 20 days, the levels were further down regulated in the irradiated (alone) as well as the combined groups (Fig. 5h). Furthermore, the levels of IL-1α and GM-CSF were also found depleted in 10 Gy alone and the combined (G003M + 10Gy) group at both the time points of study compared to tumor (alone) mice (Fig. 5i, j). Thus, G-003M induced a similar pattern of down regulation of inflammatory cytokines comparable to the Amifostine treated group (Fig. 5h–j). These findings suggest that G-003M administration not only activates anti-tumor immune response but also minimises the inflammation.

Discussion

Currently, there is no approved medical countermeasure for restoring radiation induced GI damage. Thus, radiation-induced intestinal injury is an important cause of host vulnerability during medical management of nuclear accidents or radiotherapy procedures in GI malignancies. In our previous study, we showed that two lead molecules Podophyllotoxin and rutin in combination (coded G-003M) significantly counteracted radiation induced oxidative stress and inflammation in mice intestine [21]. These collective data suggested that G-003M might play an important role in maintaining ISC pool essential for animal survival during lethal radiation exposure. Hence, the current study was primarily focussed on exploring the mechanism of G-003M mediated intestinal regeneration following radiation injury.

Radiation induced intestinal inflammation is accompanied by increased infiltration of immune cells (Neutrophils, T cell, B cell) into the intestinal venules along the crypt–villus axis [30]. This requires the participation of adhesion molecules (ICAM-1 and V-CAM-1) expressed on the endothelial cells' surface for facilitating immune cell extravasation [31]. Previous reports indicate that ICAM-1 [32] supports early leukocyte recruitment, whereas VCAM-1 [33] is the key molecular determinant of leukocyte recruitment at late time points following abdominal irradiation. Since these adhesion molecules critically regulate immune response at the inflammatory sites, modulating its expression

might be a crucial therapeutic target for minimizing radiation induced inflammation. Our findings demonstrated significant infiltration of Gr-1$^+$ (Myeloid lineage), CD3$^+$ (T-cell) and CD19$^+$ (B-cell) immune cells along with concomitant up regulation of ICAM-1 and VCAM-1cells in the intestinal venules of mice following radiation exposure (Fig. 1). Interestingly, G-003M administration restricted the radiation induced infiltration of these immune cells in mice intestine by early time point following TBI. This feature was possible due to downregulation of ICAM-1 and VCAM-1 expression in the intestinal endothelium of G-003M + TBI treated mice. Importantly, G-003M + Bay11-7082 treated group also exhibited a similar pattern of restricted immune cell infiltration comparable to the G-003M cohorts. This proves that G-003M and Bay11-7082 [34] exhibited its anti-inflammatory effects mainly through combined blockade of NF-κB activation [21] and its restricted nuclear translocation in mice intestine. This interplay of G-003M and Bay11-7082 exhibited a dominant role in reducing the expression of these adhesion molecules, thereby minimizing intestinal inflammation. Our studies proved NF-κB inactivation as the predominant mechanism underlying G-003M mediated inhibition of intestinal inflammation.

Here, for the first time we demonstrated that administration of G-003M amplified the Lgr5 expressing intestinal crypt stem cell population and restored GI functionalities through improved mice survival. Significant increase in crypt depth and proliferative index, reduced crypt apoptosis, increased presence of regenerative crypt microcolonies and maintenance of the mean crypt-villi length cumulatively assisted in G-003M mediated intestinal mucosa regeneration after lethal irradiation (Figs. 1, 2). These histological alterations evident on the small intestine of G-003M pre-treated mice accelerated the restoration of normal absorptive function of the intestine.

Several in vivo approaches have elucidated the role of different mediatory components of Wnt/β-catenin signaling in intestinal epithelium reconstitution and homeostasis [35–37]. Wnt/β-catenin signaling also plays a decisive role in cell survival as knockdown of Wnt signals by XAV939 has shown to promote cellular apoptosis [38]. On a similar note, our results also suggested the induction of Wnt signals to be a critical protective mechanism during intestinal repair in the G-003M treated group after radiation exposure (Fig. 2). In our knockdown experiments, we found that G-003M could not inhibit radiation induced animal mortality from GI injury in the groups administered with the small molecule inhibitor XAV939. This was possibly due to greater incidence of cellular apoptosis, DNA damage and fewer numbers of regenerative or viable crypts which compromised the overall functionality of the intestine leading to mice mortality (Figs. 1, 4). Hence, G-003M treatment led to restoration of overall structural and absorptive function of the intestine (Figs. 1, 2, 3, 4). At a molecular level, G-003M treatment enhanced the transactivation of Wnt target effectors due to increased nuclear levels of β-catenin in the irradiated crypt cells. Prominent Wnt target effectors that are induced in G-003M-treated animals are Survivin, Nanog and c-Myc, which mainly mediate ISCs expansion, differentiation, intestinal homeostasis and cell arrangement along the crypt villus axis following TBI [39–41] (Fig. 3d). Additionally, we found a profound amplification of Lgr5^{+ve}expressing crypt base columnar cells, signifying the proliferation and expansion of mice ISCs [1] in G-003M treated cohorts. These findings alongwith the histological observations of G-003M mediated enhanced crypt regeneration and intestinal reconstitution led to better animal survival [21] than other reported radioprotective agents like pyridoxamine [42], 17-DMAG [43], orientin and vicenin [44], Triphala [45], Aegle marmelos (L.) Correa [46] against similar radiation doses.

Our previous study [21] have reported the differential radioprotective ability of G-003M in normal versus tumor tissues in mice. Similarly, numerous other radioprotective agents like Amifostine, R-Spondin-1, Curcumin [47–49] have also been amply reported for delivering differential protection in normal versus tumor tissues. Hence, to extrapolate our previous findings for clinical radiotherapy application, we compared the anti-tumor effects of G-003M with Amifostine (FDA approved radioprotector for clinical radiotherapy). Interestingly, our data showed that the combined treatment G-003M + IR was marginally more effective than Amifostine + IR in arresting tumor growth (Fig. 5), though difference was non-significant.

Ionising radiation exerts its anti-cancer effects by directly killing the tumor cells and immunomodulating the tumor phenotypes to pro-immunogenic [50]. Further, while total body irradiation induces pro-inflammatory responses, localised tumor irradiation on the other hand, elicits an anti-inflammatory responses that contribute to tumor growth control [51, 52]. In the present study, we demonstrated that localised tumor irradiation reduced the inflammatory response (IL-6, GM-CSF, IL-1α) (Fig. 5h–j), which was further downregulated by the combined treatment G-003M + IR. Our findings also confirmed that G-003M was marginally more potent than Amifostine in reducing inflammatory response. A shift to antitumor immune response (Th1) (Fig. 5e–g) besides decrease in inflammation was also observed in both G-003M and Amifostine treated cohorts. These findings clearly indicated the antitumor immune response potentiated by the combination treatment in mice.

IL-12 P40 plays a crucial role in regulating the antitumor immune response or abnormal inflammation upstream to the Th1 cytokines. Interestingly, at day 8 and day 20 after the combined treatment, down regulation of IL12 P40 levels in both the G-003M and Amifostine treated cohorts

led to reduction in inflammation (Fig. 5d). The reduction in IL-12P40 levels observed at 8 days after the combination treatments was not restored by 20 days in animals treated with either G-003M or Amifostine (Fig. 5d). In contrast, the upregulated IL12 P40 levels observed in the untreated tumor group at day 8 and 20 could be related to rapid tumor growth and inflammation (Fig. 5d). Briefly, our findings imply that IL-12 P70 critically up-regulates Th1 related cytokines in the animals showing tumor growth arrest, while tumor regrowth could be linked to IL-12 P40 levels.

Taken together, our findings evidently put forward that G-003M is a safe and effective countermeasure for ameliorating intestinal injuries induced by varied kind of accidental or medicinal IR exposure. Since, G-003M has shown no protective effect on tumor tissue during focal radiation therapy (Fig. 5), prophylactic use of G-003M, will certainly enhance the therapeutic ratio of radiotherapy in GI cancer patients. However, these findings need to be supported through validation of outcomes in higher animal models before proceeding for translational practice.

Methods

Experimental animals and γ-irradiation

Male C57BL/6 (6–8 weeks old) housed at the Institute's experimental animal facility were used in the study. Protocols mentioned in [21] were strictly followed for γ-irradiation of mice. Unless otherwise mentioned, each experiment was repeated three times.

Ethics statement

All the experiments carried out adhered strictly to the guidelines approved by Institutional Animal Care and Use Committee (IACUC) of our institute, Institute of Nuclear Medicine and Allied Sciences (INMAS) (INM/IAEC/2013/03, dated 06.06.2013). All efforts were made to minimize animal suffering by administering anaesthesia (intraperitoneal ketamine and xylazine 7:1 mg/ml for 100 l/mice) prior to euthanasia using 100% CO_2 asphyxiation. All the animal experimental procedures for tumor development in mice were carried out in strict accordance with the recommendations in the Guide for the Care and Use of Laboratory Animals in cancer research of United Kingdom Coordinating Committee on Cancer Research (UKCCCR) and duly approved by the Institutional Animal Care and Use Committee (IACUC). Our experiments strictly adhered to ARRIVE guidelines for in vivo animal experimentation.

Preparation of radioprotective formulation (G-003M)

The structural formula and chemo-profiles of podophyllotoxin and rutin used in preparing G-003M are mentioned in our previous study [53]. Radioprotective formulation (G-003M) was prepared according to the protocol mentioned in [21]. To determine the effective dose for in vivo radioprotective potential, G-003M was injected at different therapeutic doses 2–10 mg/kg through intramuscular route in C57BL/6J mice 60 min before total body-irradiation (TBI). Our results revealed that G-003M was maximally effective when administered at 6.5 mg/kg of mice body weight.

Immunoblot analysis

Whole cell protein was isolated based on protocol mentioned in [21] and probed with primary antibodies mice anti β-actin (1:1000 dilution, Santa-Cruz Scientific, Cat no. sc-8432), rabbit Anti-GPCR GPR49 (Lgr5) (1:1000 dilution, Abcam, Cat No ab75732), mice anti-DKK1 (1:5000 dilution, Abcam, Cat No ab61275), rabbit anti-c-Myc (1:5000 dilution, Abcam, Cat No ab32072), rabbit anti-Nanog (1:1000 dilution, Abcam, Cat No ab80892), rabbit anti-Wnt3A (1:2000 dilution, Millipore, Cat no. 09-162), rabbit anti-GAPDH (1:2000 dilution, Millipore, Cat no. ABS16), rabbit anti-β-Catenin (1:2000 dilution, Millipore, Cat No. 04-1002), rabbit anti-Survivin (1:1000 dilution, Chemicon International, Cat No.AB3611), anti-ICAM1 (1:1000 dilution, Abcam, Cat No ab25375), anti-VCAM1 (1:1000 dilution, Abcam, Cat No ab215380), rabbit anti-active Caspase-3 (1:1000, Sigma, Cat No C8487) overnight at 4 °C for western blot analysis.

Subcellular (nuclear and cytoplasmic) fractionation

Nuclear and cytoplasmic fractions from the jejunum homogenates were prepared using protocol mentioned in [21]. Examination of β-Catenin expression in nuclear and cytoplasmic fractions was done by western blotting as described above by using rabbit anti-β-Catenin (1:2000 dilution, Millipore, Cat No. 04-1002), mice anti β-Tubulin (1:1000 dilution, Santa-Cruz Scientific), anti-Lamin B polyclonal primary antibody (1:4000; Sigma Co., St. Louis, MO), and goat anti-mice and goat anti-rabbit IgG-HRP secondary antibody (1:7000; Millipore, MA, USA, Cat no. AP308P, AP307P).

Immunohistochemistry

Immunohistochemical staining was performed according to protocols mentioned in [21]. Using this protocol, intestinal tissue sections were probed using Anti-GPCR GPR49 (Lgr5) (1:100 dilution, Abcam, Cat No ab75732),

rabbit anti-β-Catenin (1:100 dilution, Millipore, Cat No. 04-1002), anti-CD3e (1:100 dilution, BD Biosciences), anti-GR-1(1:100 dilution, BD Biosciences), anti-CD19 (1:100 dilution, BD Biosciences), anti phospho-histone γH2AX Ser 139 monoclonal antibody (1:100 dilution, Millipore, Cat. no. 05-636) either for 1 h at room temperature or overnight at 4 °C.

Histology

Protocols mentioned in [21] were followed for histopathological analysis of mice jejunum.

Crypt survival assay

Regenerative/viable crypts were measured in 6–8 weeks old mice sacrificed at 24 h, 3.5th Day, 7th Day after 9 Gy irradiation using the protocol mentioned in our previous study [21].

TUNEL assay

The TUNEL staining for evaluating crypt apoptosis was performed according to protocols mentioned in our previous studies [21].

Development of tumor mice model

Tumor mice model was developed according to the protocols mentioned in our previous reports [21] with minor modifications. Mice (3–6 per group) were randomised by weight into seven experimental groups. The seven groups consist of (I) Untreated (mice with no tumor and no treatment) (II) Tumour only (mice with tumor but no treatment) (III) G-003M (tumor bearing mice treated with G-003M (6.5 mg/kg body wt) alone i.m.) (IV) IR (tumor bearing mice treated with focal irradiation of 10 Gy) (V) G-003M + IR (tumor bearing mice treated with intramuscular injection of G-003M followed by focal irradiation of 10 Gy to the tumor) (VI) Amifostine (tumor bearing mice treated with Amifostine (150 mg/kg body wt) alone i.p.) (VII) Amifostine + IR (tumorbearing mice treated with intraperitoneal injection of Amifostine followed by focal irradiation of 10 Gy to the tumor).

Tumor volume measurement

Tumor volume in mice were measured by protocols mentioned in our previous study [21].

Haematological assay in tumor bearing mice

Blood samples were collected from orbital plexus of differentially treated groups and analysed for % Lymphocytes according to protocols mentioned in our previous study [21].

Cytokine estimation in tumor bearing mice

Blood samples were collected for analysing cytokine levels of IL-6, TNF-α, GM-CSF, IL-12P70, IL-12P40, IL-2, IFN-γ and IL-1α based on protocols mentioned in [21].

Administration of amifostine

Amifostine (150 mg/kg) (kind gift from Dr. Aseem Bhatnagar) was used as a positive control for the tumor based studies. Amifostine is a well-recognized and potent radioprotector, which has been approved previously by the FDA for clinical radiotherapy [54]. It was prepared by freshly dissolving in sterile distilled water and was administered intraperitoneally 30 min prior to radiation exposure.

Administration of bay 11-7082

Bay 11-7082 (Cat no: B5556-10MG, Sigma-Aldrich) is a small molecule inhibitor of IκBα phosphorylation that leads to NF-κB inactivation [55]. The drug was reconstituted in 1% Dimethyl Sulfoxide (DMSO) and administered intraperitoneally to mice at a dose of 20 mg/kg 15 min before the administration of G-003M.

Administration of XAV939

XAV939 (Cat No. ab120897, Abcam) is a small molecule inhibitor of WNT signaling pathway. The drug was reconstituted in 1% Dimethyl Sulfoxide (DMSO) and administered intraperitoneally to mice.

Statistical analysis

All results are represented as the mean ± SD of three independent experiments. Significant differences between different treatment groups was established by one-way analysis of variance (ANOVA) using the Student–Newman–Keuls Method of pair wise multiple comparisons. Values of $p < 0.05$ were considered statistically significant. For each analysis, experimental unit was an individual animal.

Acknowledgements We extend our sincere gratitude to Dr. Ajay Kumar Singh, Director, INMAS for providing necessary infrastructure and support to accomplish this work. We also thank Dr. B.G. Roy for providing experimental animals for the study. The support from Ms

Anjali Sharma and Ms Namita Kalra for irradiation facility and flow cytometry measurements is duly acknowledged. BK, RR acknowledges UGC for the award of senior research fellowship.

Author Contributions BK MLG: Conceived, designed and performed the experiments. RR BK: Analyzed the data. RR BK: Contributed reagents/materials/analysis tool. MLG BK: Wrote the paper.

Funding This work was funded by the grant INM-313 from Defence Research & Development Organization (DRDO), Ministry of Defence, Govt. of India. BK, RR acknowledges University Grants Commission (UGC), Governtment of India for the award of senior research fellowship. The funding agencies had no role in study design, data collection and analysis, decision to publish, or preparation of the manuscript.

Compliance with ethical standards

Conflict of interest The authors declared no conflict of interest regarding the work presented in the manuscript.

References

1. Barker N, Van Es JH, Kuipers J, Kujala P, Van Den Born M, Cozijnsen M, Haegebarth A, Korving J, Begthel H, Peters PJ (2007) Identification of stem cells in small intestine and colon by marker gene Lgr5. Nature 449(7165):1003
2. Zhu L, Gibson P, Currle DS, Tong Y, Richardson RJ, Bayazitov IT, Poppleton H, Zakharenko S, Ellison DW, Gilbertson RJ (2009) Prominin 1 marks intestinal stem cells that are susceptible to neoplastic transformation. Nature 457(7229):603
3. Sangiorgi E, Capecchi MR (2008) Bmi1 is expressed in vivo in intestinal stem cells. Nat Genet 40(7):915
4. Potten CS, Kovacs L, Hamilton E (1974) Continuous labelling studies on mouse skin and intestine. Cell Prolif 7(3):271–283
5. Cheng H, Leblond C (1974) Origin, differentiation and renewal of the four main epithelial cell types in the mouse small intestine III. Entero-endocrine cells. Am J Anat 141(4):503–519
6. Monti P, Wysocki J, Van der Meeren A, Griffiths N (2005) The contribution of radiation-induced injury to the gastrointestinal tract in the development of multi-organ dysfunction syndrome or failure. Br J Radiol (1):89–94
7. Gudkov AV, Komarova EA (2010) Pathologies associated with the p53 response. Cold Spring Harb Perspect Biol 2(7):a001180
8. Gregorieff A, Clevers H (2005) Wnt signaling in the intestinal epithelium: from endoderm to cancer. Genes Dev 19(8):877–890
9. Leedham S, Brittan M, McDonald S, Wright N (2005) Intestinal stem cells. J Cell Mol Med 9(1):11–24
10. Salin C, Samanta N, Goel H (2001) Protection of mouse jejunum against lethal irradiation by *Podophyllum hexandrum*. Phytomedicine 8(6):413–422
11. Bump E, Malaker K (1998) Radioprotectors: Chemical. biological and clinical perspective. CRC Press, Boca Raton
12. Nair CK, Parida DK, Nomura T (2001) Radioprotectors in radiotherapy. J Radiat Res 42(1):21–37
13. De Souza C, Santini G, Marino G, Nati S, Congiu A, Vigorito A, Damasio E (2000) Amifostine (WR-2721), a cytoprotective agent during high-dose cyclophosphamide treatment of non-Hodgkin's lymphomas: a phase II study. Braz J Med Biol Res 33(7):791–798
14. Hosseinimehr SJ (2007) Trends in the development of radioprotective agents. Drug Discov Today 12(19–20):794–805
15. Maisin J-R (1998) Bacq and Alexander award lecture chemical radioprotection: past, present and future prospects. Int J Radiat Biol 73(4):443–450
16. Weiss JF, Landauer MR (2003) Protection against ionizing radiation by antioxidant nutrients and phytochemicals. Toxicology 189(1–2):1–20
17. Jagetia GC (2007) Radioprotective potential of plants and herbs against the effects of ionizing radiation. J Clin Biochem Nutr 40(2):74–81
18. Gupta M, Agrawala P, Kumar P, Devi M, Soni N, Tripathi R (2008) Modulation of gamma radiation-inflicted damage in Swiss albino mice by an alcoholic fraction of *Podophyllum hexandrum* rhizome. J Med Food 11(3):486–492
19. Sankhwar S, Gupta ML, Gupta V, Verma S, Suri KA, Devi M, Sharma P, Khan EA, Alam MS (2011) Podophyllum hexandrum-mediated survival protection and restoration of other cellular injuries in lethally irradiated mice. Evidence-Based Complementary and Alternative Medicine. https://doi.org/10.1093/ecam/nep061
20. Lata M, Prasad J, Singh S, Kumar R, Singh L, Chaudhary P, Arora R, Chawla R, Tyagi S, Soni N (2009) Whole body protection against lethal ionizing radiation in mice by REC-2001: a semi-purified fraction of Podophyllum hexandrum. Phytomedicine 16(1):47–55
21. Kalita B, Ranjan R, Singh A, Yashavarddhan M, Bajaj S, Gupta ML (2016) A combination of podophyllotoxin and rutin attenuates radiation induced gastrointestinal injury by negatively regulating NF-κB/p53 signaling in lethally irradiated mice. PLoS ONE 11(12):e0168525
22. Verma S, Kalita B, Bajaj S, Prakash H, Singh AK, Gupta ML (2017) a combination of Podophyllotoxin and rutin alleviates radiation-induced Pneumonitis and Fibrosis through Modulation of lung inflammation in Mice. Front Immunol 8:658
23. Singh A, Yashavarddhan M, Kalita B, Ranjan R, Bajaj S, Prakash H, Gupta ML (2017) Podophyllotoxin and rutin modulates ionizing radiation-induced oxidative stress and apoptotic cell death in mice bone marrow and spleen. Front Immunol 8:183
24. Potten CS, Booth D, Haley J (1997) Pretreatment with transforming growth factor beta-3 protects small intestinal stem cells against radiation damage in vivo. Br J Cancer 75(10):1454
25. Rosenberg SA, Restifo NP, Yang JC, Morgan RA, Dudley ME (2008) Adoptive cell transfer: a clinical path to effective cancer immunotherapy. Nat Rev Cancer 8(4):299
26. Manetti R, Parronchi P, Giudizi MG, Piccinni M, Maggi E, Trinchieri G, Romagnani S (1993) Natural killer cell stimulatory factor (interleukin 12 [IL-12]) induces T helper type 1 (Th1)-specific immune responses and inhibits the development of IL-4-producing Th cells. J Exp Med 177(4):1199–1204
27. Seder RA, Gazzinelli R, Sher A, Paul WE (1993) Interleukin 12 acts directly on CD4 + T cells to enhance priming for interferon gamma production and diminishes interleukin 4 inhibition of such priming. Proc Natl Acad Sci 90(21):10188–10192
28. Magram J, Connaughton SE, Warrier RR, Carvajal DM, Wu C-y, Ferrante J, Stewart C, Sarmiento U, Faherty DA, Gately MK (1996) IL-12-deficient mice are defective in IFNγ production and type 1 cytokine responses. Immunity 4(5):471–481
29. Lu H, Ouyang W, Huang C (2006) Inflammation, a key event in cancer development. Mol Cancer Res 4(4):221–233
30. Qiu W, Wang X, Buchanan M, He K, Sharma R, Zhang L, Wang Q, Yu J (2013) ADAR1 is essential for intestinal homeostasis and stem cell maintenance. Cell Death Dis 4(4):e599
31. Springer TA (1994) Traffic signals for lymphocyte recirculation and leukocyte emigration: the multistep paradigm. Cell 76(2):301–314
32. Hallahan D, Kuchibhotla J, Wyble C (1996) Cell adhesion molecules mediate radiation-induced leukocyte adhesion to the vascular endothelium. Cancer Res 56(22):5150–5155

33. Mollà M, Gironella M, Miquel R, Tovar V, Engel P, Biete A, Piqué JM, Panés J (2003) Relative roles of ICAM-1 and VCAM-1 in the pathogenesis of experimental radiation-induced intestinal inflammation. Int J Radiat Oncol Biol Phys 57(1):264–273
34. Juliana C, Fernandes-Alnemri T, Wu J, Datta P, Solorzano L, Yu J-W, Meng R, Quong AA, Latz E, Scott CP (2010) The anti-inflammatory compounds parthenolide and Bay 11-7082 are direct inhibitors of the inflammasome. J Biol Chem. https://doi.org/10.1074/jbc.M109.082305
35. Korinek V, Barker N, Moerer P, van Donselaar E, Huls G, Peters PJ, Clevers H (1998) Depletion of epithelial stem-cell compartments in the small intestine of mice lacking Tcf-4. Nat Genet 19(4):379
36. Kuhnert F, Davis CR, Wang H-T, Chu P, Lee M, Yuan J, Nusse R, Kuo CJ (2004) Essential requirement for Wnt signaling in proliferation of adult small intestine and colon revealed by adenoviral expression of Dickkopf-1. Proc Natl Acad Sci 101(1):266–271
37. Pinto D, Gregorieff A, Begthel H, Clevers H (2003) Canonical Wnt signals are essential for homeostasis of the intestinal epithelium. Genes Dev 17(14):1709–1713
38. Tian X-H, Hou W-J, Fang Y, Fan J, Tong H, Bai S-L, Chen Q, Xu H, Li Y (2013) XAV939, a tankyrase 1 inhibitior, promotes cell apoptosis in neuroblastoma cell lines by inhibiting Wnt/β-catenin signaling pathway. J Exp Clin Cancer Res 32(1):100
39. Kim PJ, Plescia J, Clevers H, Fearon ER, Altieri DC (2003) Survivin and molecular pathogenesis of colorectal cancer. The Lancet 362(9379):205–209
40. Zhang J, Wang X, Chen B, Xiao Z, Li W, Lu Y, Dai J (2010) The human pluripotency gene NANOG/NANOGP8 is expressed in gastric cancer and associated with tumor development. Oncol Lett 1(3):457–463
41. Bettess MD, Dubois N, Murphy MJ, Dubey C, Roger C, Robine S, Trumpp A (2005) c-Myc is required for the formation of intestinal crypts but dispensable for homeostasis of the adult intestinal epithelium. Mol Cell Biol 25(17):7868–7878
42. Thotala D, Chetyrkin S, Hudson B, Hallahan D, Voziyan P, Yazlovitskaya E (2009) Pyridoxamine protects intestinal epithelium from ionizing radiation-induced apoptosis. Free Radic Biol Med 47(6):779–785
43. Lu X, Nurmemet D, Bolduc DL, Elliott TB, Kiang JG (2013) Radioprotective effects of oral 17-dimethylaminoethylamino-17-demethoxygeldanamycin in mice: bone marrow and small intestine. Cell Biosci 3(1):36
44. Uma Devi P, Ganasoundari A, Vrinda B, Srinivasan K, Unnikrishnan M (2000) Radiation protection by the ocimum flavonoids orientin and vicenin: mechanisms of action. Radiat Res 154(4):455–460
45. Jagetia GC, Baliga MS, Malagi K, Kamath MS (2002) The evaluation of the radioprotective effect of triphala (an ayurvedic rejuvenating drug) in the mice exposed to γ-radiation. Phytomedicine 9(2):99–108
46. Jagetia GC, Venkatesh P, Archana P, Krishnanand BR, Baliga MS (2006) Effects of *Aegle marmelos* (L.) Correa on the peripheral blood and small intestine of mice exposed to gamma radiation. J Environ Pathol Toxicol Oncol 25 (4)
47. Yuhas JM (1980) Active versus passive absorption kinetics as the basis for selective protection of normal tissues by S-2-(3-aminopropylamino)-ethylphosphorothioic acid. Cancer Res 40(5):1519–1524
48. Bhanja P, Saha S, Kabarriti R, Liu L, Roy-Chowdhury N, Roy-Chowdhury J, Sellers RS, Alfieri AA, Guha C (2009) Protective role of R-spondin1, an intestinal stem cell growth factor, against radiation-induced gastrointestinal syndrome in mice. PLoS ONE 4(11):e8014
49. Goel A, Aggarwal BB (2010) Curcumin, the golden spice from Indian saffron, is a chemosensitizer and radiosensitizer for tumors and chemoprotector and radioprotector for normal organs. Nutr Cancer 62(7):919–930
50. Lumniczky K, Sáfrány G (2015) The impact of radiation therapy on the antitumor immunity: local effects and systemic consequences. Cancer Lett 356(1):114–125
51. Fedoročko P, Egyed A, Vacek A (2002) Irradiation induces increased production of haemopoietic and proinflammatory cytokines in the mice lung. Int J Radiat Biol 78(4):305–313
52. Frey B, Rubner Y, Wunderlich R, Weiss E-M, Pockley G, Fietkau A, R, S Gaipl U (2012) Induction of abscopal anti-tumor immunity and immunogenic tumor cell death by ionizing irradiation-implications for cancer therapies. Curr Med Chem 19(12):1751–1764
53. Dutta A, Gupta M, Kalita B (2015) The combination of the active principles of Podophyllum hexandrum supports early recovery of the gastrointestinal system via activation of Nrf2-HO-1 signaling and the hematopoietic system, leading to effective whole-body survival in lethally irradiated mice. Free Radic Res 49(3):317–330
54. Singh VK, Romaine PL, Seed TM (2015) Medical countermeasures for radiation exposure and related injuries: characterization of medicines, FDA-approval status and inclusion into the strategic national stockpile. Health Phys 108(6):607
55. Pierce JW, Schoenleber R, Jesmok G, Best J, Moore SA, Collins T, Gerritsen ME (1997) Novel inhibitors of cytokine-induced IκBα phosphorylation and endothelial cell adhesion molecule expression show anti-inflammatory effects in vivo. J Biol Chem 272(34):21096–21103